

Long Lu
Rucheng Wang
Fanrong Chen
Jiyue Xue
Peihua Zhang
Jianjun Lu

Element mobility during pyrite weathering: implications for acid and heavy metal pollution at mining-impacted sites

Received: 25 January 2005
Accepted: 3 August 2005
Published online: 5 October 2005
© Springer-Verlag 2005

L. Lu · F. Chen (✉)
Guangzhou Institute of Geochemistry,
Chinese Academy of Sciences, Guangzhou
510640, People's Republic of China
E-mail: frchen@gig.ac.cn
Tel.: +86-20-85290291
Fax: +86-20-85290130

L. Lu
The Key Laboratory of Poyang Lake
Ecology and Bio-resource Utilization,
Nanchang University, Nanchang 330029,
People's Republic of China

R. Wang · J. Xue · P. Zhang · J. Lu
Department of Earth Sciences, Nanjing
University, Nanjing 210093, People's
Republic of China

Abstract Based on back scattered electron images and electron microprobe analysis results, four alteration layers, including a transition layer, a reticulated ferric oxide layer, a nubby ferric oxide layer and a cellular ferric oxide layer, were identified in the naturally weathering products of pyrite. These layers represent a progressive alteration sequence of pyrite under weathering conditions. The cellular ferric oxide layer correlates with the strongest weathering phase and results from the dissolution of nubby ferric oxide by acidic porewater. Leaching coefficient was introduced to better express the response of element mobility to the degree of pyrite weathering. Its variation shows that the mobility of S, Co and Bi is stronger than As, Cu and Zn. Sulfur in pyrite is oxidized to sulfuric acid

and sulfate that are basically released into to porewater, and heavy metals Co and Bi are evidently released by acid dissolution. As, Cu and Zn are enriched in ferric oxide by adsorption and by co-precipitation, but they would re-release to the environment via desorption or dissolution when porewater pH becomes low enough. Consequently, Co, Bi, As, Cu and Zn may pose a substantial impact on water quality. Considering that metal mobility and its concentration in mine waste are two important factors influencing heavy metal pollution at mining-impacted sites, Bi and Co are more important pollutants in this case.

Keywords Environmental implications · Element mobility · Pyrite weathering

Introduction

The major environmental problems confronting the mining industry is the generation of acid mine drainage (AMD) upon exposure of sulfide minerals in mining wastes to atmospheric conditions. AMD is often characterized by low pH and high concentration of heavy metals and, thus, may pose a potential risk to the ecological environment. Pyrite is one of the most common minerals in mine tailings and waste rocks from metal deposits. When weathering, pyrite releases acid and heavy metals as do other sulfides. Nesbitt and Muir (1994) believed that pyrite is the main contributor of

acid and heavy metals from mine wastes. Therefore, the oxidation of pyrite has long been of major interest in scientific communities to estimate the long-time loading of acid and heavy metals from mine wastes to the environment (Mckibben and Barnes 1986; Karthe et al. 1993; Rimstidt and Newcomb 1993; Nesbitt and Muir 1994; Pratt et al. 1994a, b; Williamson and Rimstidt 1994; Schaufuss et al. 1998). However, much less attention has been paid to the element mobility associated with pyrite weathering.

Frau (2000) and Benvenuti et al. (2000) investigated the main secondary minerals in mine waste and found that sulfate minerals, such as jarosite, gypsum,

melanterite, and oxides or hydroxides of ferric iron, were developed, in turn, under weathering conditions. Based on porewater profiles, leaching experiments and chemical extraction, etc., Jurjovec et al. (2002), Al et al. (1997, 2000), McGregor et al. (1998), Blowes and Jambor (1990) and Dubrovsky (1986) have examined heavy metal mobility during tailing weathering. The element release during pyrite weathering was evaluated by analyzing the composition of surface layers, which represent progressive alteration products of pyrite under ambient conditions. This research was designed to reveal the mobility of Fe, S and heavy metals as pyrite alteration proceeds and to better understand the mechanism of heavy metal release, which provides an insight into the long-term environmental impacts of mine waste. In addition, this paper presents an alternative way to assess the element mobility in an alteration system where no element is considered immobile.

Site description

The Jiguanshan waste-rock pile is 12 km east of Tongling City, Anhui Province, beside the Yangzhi River. The pile has received a volume of approximately 5,000,000 m³ mining waste from the Jiguanshan pyrite mine since 1958. The mining waste consists of pyrite (~10 wt%), other sulfide minerals (less than 0.5 wt%), and nonsulfide minerals (~90 wt%). The most abundant nonsulfide minerals are quartz, feldspar, pyroxene, clay minerals and about 5–7 wt% calcite. The ore of the Jiguanshan mine is a massive pyrite ore and is mined to extract sulfur. Field investigation, optic microscope observation, and X-ray diffraction spectra (XRD) show that the massive ores consist of pyrite with little other minerals.

Materials and methods

Samples were collected from 50 cm depth at different locations of the Jiguanshan waste rock pile. The massive pyrite ores have developed an alteration shell of a few millimeters to a few centimeters in thickness. XRD studies show that the shells are mainly goethite with minor lepidocrocite and hematite.

Four of the massive pyrite ore samples (A, B, C, D) were selected, and polished cross sections were made. Samples A and C were weakly weathered, while samples B and D were strongly weathered. In samples B and D, ferric oxide is the dominant phase, with pyrite occurring as a tiny residual core surrounded by alteration products.

The chemical composition of natural pyrite and its alteration products was determined by JXA 8800M electron probe X-ray Micro-Analyzer made by JEOL.

The electron beam was accelerated at a voltage of 20 kV. The observation of the back scattered electron (BSE) image for pyrite and its weathering products was also performed on the instrument. The results of electron micro-probe analysis (EMPA) are presented in Table 1.

Element mobility index:leaching coefficient

When discussing the element mobility associated with silicate weathering and wall-rock alteration, enriching coefficient (F) or the variance of element concentration (ΔC) is usually used to estimate the mobility of elements and can be calculated by the following equation (Diao and Wen 1999; Gao et al. 1999):

$$F = \frac{C_i^a - C_i^0}{C_i^0} \times 100\%, \quad (1)$$

$$\Delta C = C_i^a - C_i^0, \quad (2)$$

where C_i^0 is the average concentration of element i in the primary mineral, and C_i^a denotes the average concentration of element i in the weathering product. The estimate is based on the assumption that the total mass of the solid phases is kept constant during alteration. However, this assumption is not valid for pyrite weathering as a result of sulfur release from, and the addition of oxygen and water into, the secondary phases of pyrite. The mass transport will result in dilution or enriching effect on other elements. For example, when FeS_2 is oxidized into $\text{FeO}_{1.5}$ in the reaction of $\text{FeS}_2 \rightarrow \text{FeO}_{1.5}$, the total mass changes during the reaction, which makes the Fe concentration change from 46.67 to 70.0 wt% although Fe is neither added in nor leached out. Likewise, in the process of $\text{Fe}_{0.5}\text{S} \rightarrow \text{Fe}_{2/3}\text{SO}_4$, 53.33 wt% S in FeS_2 is transformed to 24.00 wt% S in $\text{Fe}_{2/3}\text{SO}_4$ due to the addition of oxygen into the resultant. Thus, if the mobility of Fe and S is represented by F or ΔC , there would be a false conclusion that Fe is significantly enriched in the first case and S is leached in the second case.

Ti has been assumed to be a stable element that is not transported during alteration (Zhou et al. 1994; Wang et al. 1998; Diao and Wen 1999; Ma and Liu 1999), based on which Zhou et al. (1994) and Wang et al. (1998) estimated the mass transport of other elements during hydrothermal wall-rock alteration. This method can eliminate the influence of total mass change on element content. However, titanium concentration in these samples is commonly below EPMA detection limit and cannot be used as the criterion of element mobility.

In this study, an equivalent coefficient (q) was introduced, based on which equivalent calibration was made to eliminate the dilution/enriching effect on the element of interest caused by the mass transport of other elements. By this calibration, the abundance of a specific

Table 1 Elements contents in pyrite and its various alteration layers (wt% of metal atom)

Layer ^a	n ^b	S	Fe	As	Sb ^c	Cu	Pb	Zn	Cd	Co	Ni	Mn	Bi	Ti
Apm	5	52.56	45.54	0.16	0.00	0.02	0.00	0.02	0.01	0.05	0.01	0.01	0.21	0.00
A3m	3	2.41	47.92	0.07	— ^d	1.18	0.08	0.26	0.01	0.00	0.00	— ^d	— ^d	— ^d
Bpm	12	52.81	46.49	0.03	0.00	0.02	0.11	0.02	0.01	0.09	0.01	0.01	0.13	0.01
B2m	5	0.1	49.48	0.35	0.00	0.02	0.04	0.38	0.01	0.06	0.00	0.00	0.01	0.00
B3m	5	0.11	51.07	0.10	0.00	0.02	0.02	0.03	0.01	0.04	0.01	0.00	0.00	0.00
B4m	4	0.05	50.92	0.09	0.00	0.04	0.04	0.10	0.00	0.06	0.01	0.01	0.01	0.00
Cpm	6	52.79	46.66	0.15	0.02	0.05	0.00	0.01	0.00	0.08	0.01	0.00	0.20	0.00
C1m	5	38.34	46.12	0.11	0.01	0.22	0.00	0.07	0.00	0.07	0.01	0.00	0.17	0.01
C1*m	4	6.71	42.40	0.70	0.06	0.78	0.08	0.21	0.01	0.05	0.01	0.04	0.04	0.00
C2m	7	2.47	46.04	0.45	0.06	0.67	0.14	0.27	0.01	0.06	0.00	0.03	0.02	0.00
C3m	4	0.98	55.68	0.32	0.04	0.72	0.14	0.34	0.01	0.06	0.00	0.04	0.00	0.01
Dpm	3	52.66	46.38	0.05	0.00	0.00	0.00	0.00	0.01	0.05	0.01	0.01	0.23	0.01
D1m	2	45.25	43.91	0.06	0.00	0.10	0.01	0.04	0.01	0.06	0.00	0.00	0.17	0.00
D1*m	2	1.30	37.79	0.21	0.01	0.16	0.01	0.03	0.01	0.01	0.00	0.00	0.11	0.00
D2m	3	0.36	49.38	0.09	0.00	0.05	0.01	0.06	0.01	0.06	0.00	0.00	0.02	0.01
D3m	6	0.09	57.47	0.25	0.01	0.11	0.01	0.06	0.01	0.05	0	0.01	0.01	0.01
D4m	11	0.08	59.02	0.19	0.00	0.03	0.03	0.09	0.01	0.04	0.00	0.00	0.02	0.01
Spm	26	52.74	46.38	0.08	0.01	0.02	0.05	0.01	0.01	0.08	0.01	0.01	0.17	0.00
S1m	7	40.32	45.485	0.09	0.01	0.19	0.00	0.06	0.00	0.07	0.00	0.00	0.17	0.00
S1*m	6	4.91	40.86	0.53	0.04	0.57	0.05	0.15	0.01	0.03	0.00	0.02	0.06	0.00
S2m	15	1.26	47.76	0.34	0.03	0.33	0.08	0.27	0.01	0.06	0.00	0.02	0.02	0.00
S3m	18	0.68	50.55	0.19	0.01	0.40	0.06	0.14	0.01	0.04	0.00	0.01	0.01	0.01
S4m	15	0.07	52.53	0.16	0.00	0.03	0.04	0.09	0.01	0.05	0.00	0.01	0.01	0.01
Detected limit		0.001	0.021	0.026	0.013	0.025	0.040	0.029	0.013	0.018	0.018	0.019	0.022	0.024

^aA, B, C, D and S are symbols of four samples and their summation, and l(or 1*), 2, 3, 4 and p after them represent four fabric types and pyrite, respectively. The symbols of *m* denote the mean content of element *i* in fabric *j*

^b *n* is the number of analysis points

^cSb, Pb, Cd, Ni, Mn and Ti are not mentioned in following paragraph as the elements contents are under detected limit.

^d— signifies the item of no detection

element, *i*, in the alteration product of pyrite is transformed into a corresponding abundance that would have been in unaltered pyrite, and the leaching coefficient of elements in the alteration process can be calculated. The calculation of the leaching coefficient (*L*) is as follows:

$$L = \frac{C_i^0 - C_i^{aj*}}{C_i^0} \times 100\%, \quad (3)$$

where C_i^0 is the average concentration of element *i* in pyrite, and C_i^{aj*} denotes the calibrated average concentration of element *i* in the alteration layer *j* of pyrite. A positive *L* value indicates leaching, and a negative value enriching.

XRD analysis and EMPA demonstrated that the alteration product of pyrite was $\text{Fe}_2\text{O}_3 \cdot n\text{H}_2\text{O}$. Thus, 1 mol (120 g) pyrite will be altered to 0.5 mol $(80 + 9n)\text{g}$ $\text{Fe}_2\text{O}_3 \cdot n\text{H}_2\text{O}$. The equivalent coefficient of elements in the weathering product was calculated according to the mass change during alteration and based on the assumptions: (1) the difference between the EMPA total and 100 wt% is the content of H_2O , and (2) the total mass of iron is constant during alteration. Although a small amount of iron may be dissolved in porewater and transported, considering that iron is a major element in pyrite and is rather immobile during weathering, no significant influence is expected on the calculation.

The equivalent calibration of element concentration in the alteration product of layers 1*, 2, 3 and 4 was conducted by the following procedures: (1) the chemical formula of the alteration product in each layer was calculated based on the first assumption using EMPA result (Table 2); (2) the equivalent coefficient for layer *j*, q_j , was determined by the molecular weight ratio of pyrite to its alteration product in layer *j* based on the second assumption; and (3) the calibrated concentration of element *i* in layer *j* was obtained by multiplying the EMPA content of the element *i* with q_j , i.e., $C_i^{aj*} = q_j C_i^a$.

The abundances of Zn in pyrite and Co, Bi in a few ferric oxide layers were below detection limits. In these cases, their abundances were set to be their respective detection limits in calculating the mobility indices. This treatment underestimates the degree of Zn enrichment and Co, Bi release, but has little influence on the general conclusions (Table 3).

Results and discussion

Alteration layers of the weathered pyrite

Four alteration layers were identified on the weathered pyrite, each with specific structural and compositional characteristics: transition layer, reticulated ferric oxide layer, nubby ferric oxide layer and cellular ferric oxide

Table 2 The chemical formula and equivalent coefficients of layer 1* to 4

Layer	Chemical formula	Equivalent coefficient	Layer	Chemical formula	Equivalent coefficient
1*	$\text{Fe}_2\text{O}_3 \cdot 3.23\text{H}_2\text{O}$	0.909	3	$\text{Fe}_2\text{O}_3 \cdot 2.91\text{H}_2\text{O}$	0.885
2	$\text{Fe}_2\text{O}_3 \cdot 3.23\text{H}_2\text{O}$	0.909	4	$\text{Fe}_2\text{O}_3 \cdot 2.81\text{H}_2\text{O}$	0.877

Fig. 1 BSE images of four fabric types in pyrite weathered products. **a** Three fabric types in weathered products, **b** cellular fabric type. In **a**: *p* pyrite, *1* inner transition zone, *1** outer transition zone, *2* reticulation-nervation ferric oxide, *3* nubby ferric oxide. In **b**: *dr* dissolved caves, *br* ferric oxide

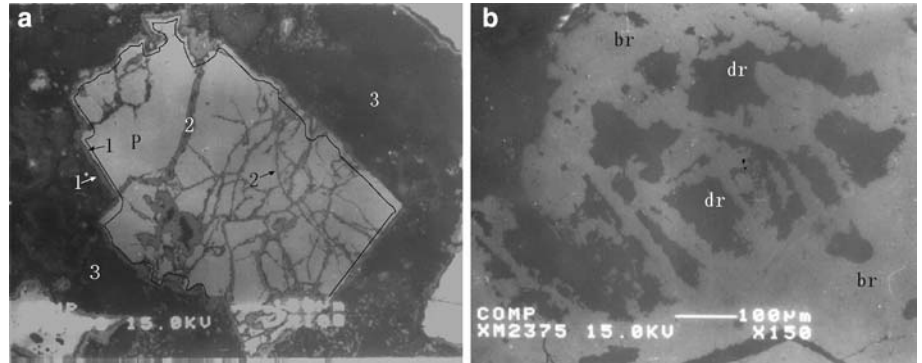
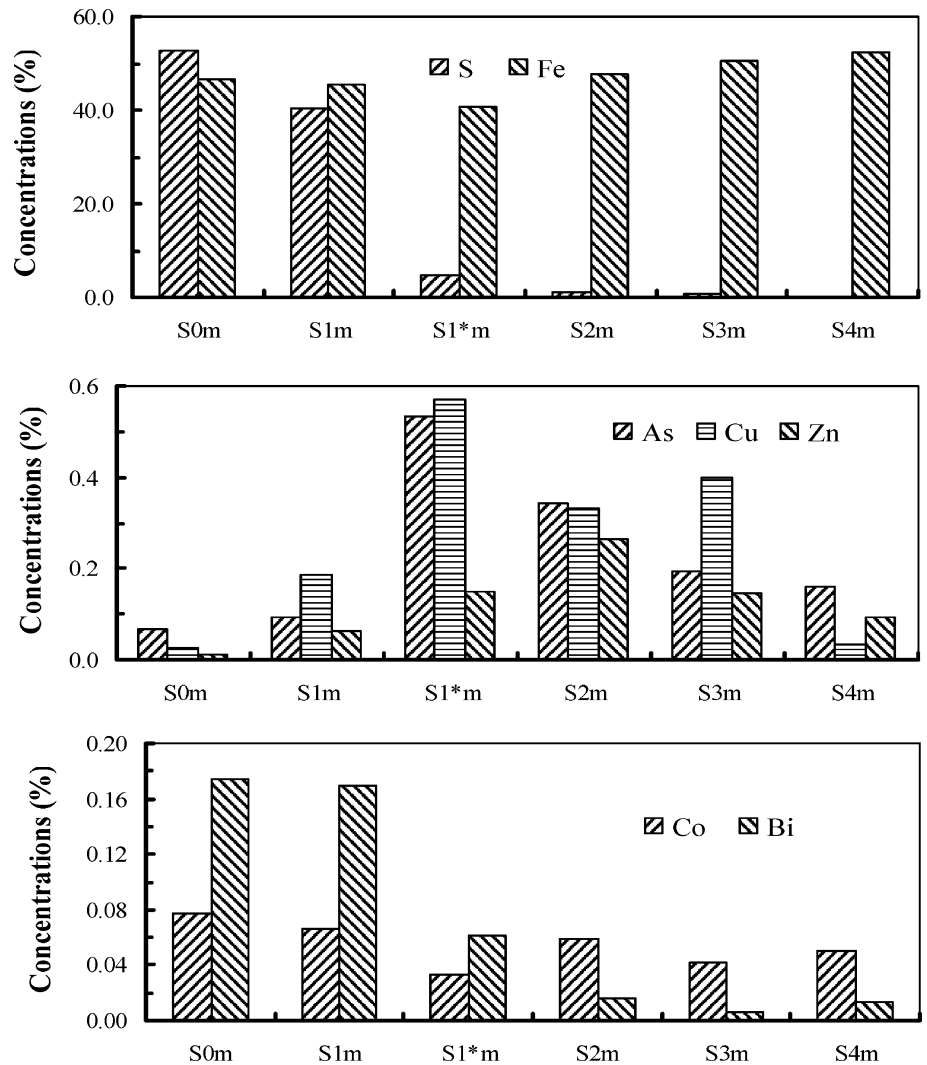


Fig. 2 Changes of element mean contents in pyrite and its various alteration layers. (Symbols are the same as in Table 1)



layer (Fig. 1). The transition layer is the inner layer that is close to fresh pyrite, where pyrite is partially altered to ferric oxide with the fraction of ferric oxide increasing outward (including inner transition layer—layer 1 and outer transition layer—layer 1*). The reticulated ferric oxide layer is characterized by the web-like distribution of ferric oxide veinlets. The thickness of this layer is usually $< 50 \mu\text{m}$ (layer 2). The characteristic of nubby ferric oxide layer is that ferric oxide forms nodules, with the layer thickness usually $> 200 \mu\text{m}$ (layer 3). In the cellular ferric oxide layer, a lot of tafoni (honey-like caves) develop in ferric oxide nodules. The diameter of the caves is usually in the range of $50\text{--}80 \mu\text{m}$ (layer 4). The authors consider these fabric layers represent a progressive weathering sequence of pyrite in light of their distribution and chemical composition. Each layer correlates with a specific alteration phase, and the cellular fabric layer forms in the last weathering phase of this sequence. Samples A and C lack the cellular fabric layer because of their weak weathering (Table 1).

The stability of the secondary Fe-rich minerals is controlled by pH, and these minerals can partially be dissolved under low pH conditions (Bigham et al. 1992; Luther 1987). Previous researches have indicated that the pH of mine drainage is usually very low (Williams and Smith 2000; Jung 2001). The acidity of porewater in mine waste increases gradually as pyrite weathering proceeds. The acidic porewater may stay for a longer time within some micro-areas in alteration products, where a part of the ferric oxides may be dissolved, resulting in the formation of the cellular fabrics. Consequently, the authors believe that the cellular fabric layer is produced in the strongest phase of pyrite weathering.

Elements mobility and its environmental effect

Variation of the average content of elements in different layers is shown in Table 1 and Fig. 2. The leaching coefficients of the elements listed in Table 3 indicate the extent of element mobility. As shown in Fig. 2 and Table 3, the elements can be divided into two groups according to their mobility, i.e., strongly leached (S, Co and Bi) and apparently enriched (As, Cu and Zn). These results are consistent with the heavy metal mobility in tailings weathering reported by Jurjovec et al. (2002), Mcgregor et al. (1998) and Dubrovsky (1986), whose researches showed Co and Ni are more mobile than Zn, Pb and Cu based on leaching experiments and porewater profile studies.

The leaching of S increases as alteration proceeds. In the cellular ferric oxide layer, S is almost gone. The variation of leaching degree suggests that pH decreases gradually during pyrite weathering, and the high leaching coefficients suggest that the porewater in the Jiguanshan waste-rock pile would be highly acidic with

large dissolution capability. This is confirmed by the formation of the cellular ferric oxide layer and supported by the low pH (4.2) of the water in small depressions in this pile measured in September, 2000.

The leaching coefficients of Co and Bi demonstrate that they have been mobilized and transported during pyrite weathering. This observation agrees well with the proposed metal mobility sequence of $\text{Ni} = \text{Co} > \text{Zn} (= \text{Cd}) > \text{Pb} (= \text{Cr}) > \text{Cu}$ based on porewater profile and leaching experimental studies of mine tailings (Jurjovec et al. 2002; Dubrovsky 1986; Mcgregor et al. 1998; Blowes and Jambor 1990). In order to confirm the relative mobility of these elements, powders of the surface film of weathered pyrite were analyzed by ICP-MS for metal concentrations, and the results showed that the concentrations of Bi, Cd, Co and Ni are 1–2 orders of magnitude lower than As, Cu, Pb and Zn (Lu 2002). In the fresh pyrite, however, Bi and Co concentrations are not lower than those of As, Cu, Pb and Zn. These results also demonstrate the higher mobility of Bi and Co during pyrite weathering.

As compared with As, Cd, Cu, Ni, Pb and Zn, the content of Bi and Co in mine waste samples are usually low and, thus, not considered to be important pollutants in most cases (Gade et al. 2001; Jung 2001; Lee et al. 2001; Parsons et al. 2001; Benvenuti et al. 1997). In contrast, the pyrite from the Jiguanshan waste-rock pile has elevated concentrations of Bi and Co, with their mean abundances in all the studied samples (A, B, C and D) more than 1.6 times higher than those of Cd, Cu, Ni, Pb and Zn. Therefore, the elevated concentration and high mobility of Bi and Co would make them more important as pollutants than As, Cu and Zn in the mine drainage from the Jiguanshan waste rock pile.

The leaching coefficients of As, Cu and Zn indicate that these elements are immobilized in the alteration products, especially in layers 1* to 3. This result is similar to the observation by Gade et al. (2001) and Pichler et al. (2001) that these metals are dominantly retained in hydrous ferric oxide under oxidizing conditions. In the cellular ferric oxide layer, however, the leaching coefficients of As, Cu and Zn dramatically increase to a level close to or higher than that in the inner transition layer. The sharp attenuation in the enriching degree of As, Cu and Zn suggests that the elements were evidently leached in the last phase of alteration, which implies that these metals can finally be released when the medium pH becomes low enough, and could be a long-time environmental concern.

Mechanism of element transfer or transport

Sulfur in sulfide minerals is usually oxidized to sulfuric acid and sulfate during oxidative alteration (Pratt et al.

Table 3 Leaching coefficients in various alteration layers of pyrite

	S	Fe	As	Cu	Zn	Co	Bi
LA3m	95.95	6.88	-21.54	-4097.80	-1004.10	66.98	-
LB2m	99.82	3.84	-1080.16	9.15	-2044.21	42.48	83.33
LB3m	99.82	2.79	-229.82	1.40	-38.82	59.62	83.33
LB4m	99.92	3.95	-179.98	-60.75	-470.63	40.14	83.33
LC1m	27.36	1.17	24.47	-371.60	-149.10	14.48	14.95
LC1*m	88.45	11.41	-322.05	-1411.93	-567.37	48.06	83.54
LC2m	95.74	10.31	-171.57	-1205.13	-765.93	29.67	89.83
LC3m	98.36	4.94	-90.08	-1256.16	-944.50	38.44	88.76
LD1m	14.07	5.33	-6.99	-288.94	-40.63	-33.68	27.20
LD1*m	97.75	25.94	-257.25	-467.25	15.91	54.59	55.61
LD2m	99.38	3.23	-51.33	-94.14	-86.28	8.78	90.23
LD3m	99.84	1.30	-314.83	-305.70	-70.41	1.92	90.23
LD4m	99.86	-0.45	-211.93	-11.44	-173.45	20.38	90.23
LS1m	23.56	1.93	-13.26	-654.71	-118.11	15.12	2.94
LS1*m	91.55	19.92	-622.67	-2016.60	-372.94	60.57	67.91
LS2m	97.83	6.40	-364.87	-1124.91	-733.55	30.43	87.12
LS3m	98.86	3.54	-155.76	-1339.74	-341.01	51.90	87.12
LS4m	99.88	0.66	-109.34	-16.35	-184.92	43.86	87.12

L denotes leaching coefficients. Other symbols are the same as in Table 1

1994a, b). Most of the chemical species of sulfur usually dissolve in porewater, but a minor part remains in alteration products as sulfate minerals, such as jarosite and gypsum. These mineral phases control the partitioning of Fe, Ca and SO₄ between porewater and alteration products (Mcgregor et al. 1998). The high leaching coefficients of S suggest that a large amount of acid should be released due to pyrite weathering. The acid accumulation in, and the dissolution capability of the porewater increase continuously as pyrite alteration goes on, resulting in the dissolution of sulfate minerals formed previously as alteration products. Thus, the leaching coefficient of S increases gradually during pyrite weathering, and little S remains in the last phase of weathering.

The positive leaching coefficient of Co and Bi in layer 1 implies that they are released at the beginning of pyrite weathering. This observation is consistent with the previous results indicating that most Bi, Cd, Co and Ni were released from the weathering film of pyrite (Lu 2002). Hence, most of the Bi and Co was dissolved in porewater in the early stage of pyrite weathering. This conclusion is supported by the results of Dzombak and Morel (1990), who observed that at pH 6.6, only 25 and 30% of Ni and Co in their experimental system were, respectively, adsorbed onto the surface of the hydrous ferric oxide. Moreover, the mean *L* values of Co and Bi for all the sample types (A, B, C and D) increase obviously from layer 1 to layer 1*, and change little from layer 1* to layer 4. This observation suggests that most Bi and Co would be leached out in the early stage of pyrite weathering when the pH declines to a specific value, and the residual of the metals might remain immobilized even if the pH decreases further. Jurjovec et al. (2002) observed similar results in column experiment where a large amount of Co and Ni in the samples from tailings was dissolved at the plateau of pH 5.7, and

little of the metals were leached afterwards when the pH decreased from 5.7 to 1.

The amount of As, Cu and Zn in pyrite cannot account for the metals contained in the alteration products (Table 1). Conceivably, surface absorption and/or co-precipitation may contribute to the immobilization of the metals (Morin et al. 1999; Benvenuti et al. 1997; Mcgregor et al. 1998; Nickson et al. 2000; Simma et al. 2000; Yu and Heo 2001). The contents of Cu, Pb, Zn and Ag in pyrite coatings increased at the expense of those in porewater with increasing pH, and the distribution of metals between mineral surface and porewater as a function of pH can be explained by adsorption models (Al et al. 1997). Previous researches have shown that Cu, Pb, Zn, Cd, Co, Ni etc. can observably be adsorbed on hydrous ferric oxide (Wu et al. 1997; Parkman et al. 1999; Dzombak and Morel 1990) and Fe, Mn oxide in soil (Morin et al. 1999), but their adsorption density depends on the temperature and the pH of medium solution (Wu et al. 1996). Obviously, surface adsorption and co-precipitation immobilize Cu and Zn dissolved in porewater and contribute to the elevated concentration of Cu and Zn in the alteration products of pyrite, but they are desorbed and dissolved as pH of porewater is low enough. On the other hand, the enrichment of As in the weathering products of pyrite cannot be explained using the adsorption model, because it dominantly occurs in oxic porewater as arsenate anions with their adsorption behavior quite different from cationic ions of metals (Al, et al. 1997). Thus, the mobility of As is likely to be controlled by the precipitation and co-precipitation mechanisms. Therefore, the significant enrichment of As, Cu and Zn in layers 1 to 3 should result from mass transfer by both adsorption (for Cu, Zn), co-precipitation and precipitation during pyrite weathering, and the dramatic increase of the leaching

coefficient of As, Cu and Zn in cellular ferric oxide is the result of dissolution and/or desorption.

Conclusions

Four alteration layers, i.e., transition layer, reticulated ferric oxide layer, nubby ferric oxide layer, and cellular ferric oxide layer, are gradually developed during pyrite weathering. These layers constitute a progressive weathering sequence of pyrite.

Variations in leaching coefficients indicate that: (1) S, Co and Bi are more mobile than As, Cu and Zn, and would significantly be released in the early stages of pyrite weathering, (2) As, Cu, Zn are immobilized by the alteration products in layers 1 to 3, but obviously leached in layer 4 due to the lower pH of porewater in the last phase of weathering, and (3) Acid, Co and Bi may be among the major pollutants associated with pyrite weathering in the studied site,

while As, Cu and Zn may pose a long-time threat to the environment.

As is well known, S can easily be oxidized into sulfuric acid and sulfate, and cause acid pollution. The mobile characteristics of Co and Bi during pyrite weathering are supported by porewater chemistry and leaching experiments of mine tailings. Adsorption and/or co-precipitation are proposed to be the major mechanisms for the immobilization of As, Cu, Zn by the weathering products of pyrite; and, thus, the release of these elements in the last phase of alteration should be caused by the host phase dissolution and desorption at low pH values.

Acknowledgements This study was financially supported by the National Natural Science Foundation of China, (40025209) and the Hundred Talents Program of Chinese Academy of Sciences (2000[254]). EMPA and BSE images were completed in the State Key Laboratory for Mineral Deposit Research, Nanjing University. The authors would like to express heartfelt thanks to Dr. X.D. Li at the Hong Kong Polytechnic University for his constructive comments.

References

- Al TA, Blowes DW, Martin JL, Cabri LJ, Jambor JL (1997) Aqueous geochemistry and analysis of pyrite surface in sulfide-rich mine tailings. *Geochim Coschim Acta* 61:2353–2366
- Al TA, Martin JL, Blowes DW (2000) Carbonate-mineral/water interactions in sulfide-rich mine tailings. *Geochim Coschim Acta* 64:3933–3948
- Benvenuti M, Mascaro I, Corsini F (1997) Mine waste dumps and heavy metal pollution in abandoned mining district of Boccheggiano (Southern Tuscany, Italy). *Environ Geol* 30:238–243
- Benvenuti M, Mascaro I, Corsini F, Ferrari M, Lattanzi P, Parrini P, Costagliola P, Tanelli G (2000) Environmental mineralogy and geochemistry of waste dumps at the Pb (Zn)-Ag Bottino mine, Apuane Alps, Italy. *Eur J Mineral* 12:441–453
- Bigham JM, Schwertmann U, Carlson L (1992) In: Skinner HCW, Fitzpatrick RW (eds) *Biomineralization: processes of iron and manganese*, supplement 21. Catena, Gremlingen-Destedt, pp 219–232
- Blowes DW, Jambor JL (1990) The pore-water geochemistry and the mineralogy of the vadose zone of sulfide tailings, Waite Amulet, Quebec, Canada. *Appl Geochem* 5:327–346
- Diao GY, Wen QZ (1999) The migration series of major elements during loess pedogenesis (in Chinese with English abstract). *Geol Geochem* 27:21–26
- Dubrovsky NM (1986) Geochemical evolution of inactive pyritic tailings in the Elliot Lake Uranium District. Ph. D. thesis, University of Waterloo
- Dzombak DA, Morel FMM (1990) Surface complexation modeling: Hydrous ferric oxide. Wiley, New York
- Frau F (2000) The formation-dissolution cycle of melanterite at the abandoned pyrite mine of Genna Luas in Sardinia, Italy: environmental implications. *Mineral Mag* 64:995–1006
- Gade B, Pollmann H, Heindl A, Westermann H (2001) Long-term behavior and mineralogical reactions in hazardous waste landfills: a comparison of observation and geochemical modeling. *Environ Geol* 40:248–256
- Gao B, Ma DS, Liu LW (1999) The immobile elements identification and mass transfer in the geochemical process of wall-rock alteration (in Chinese with English abstract). *Acta Geologica Sinica* 73:272–277
- Jung MC (2001) Heavy metal contamination of soils and waters in and around the Imcheon Au-Ag mine, Korea. *Appl Geochem* 16:1369–1375
- Jurjovec J, Ptacek CJ, Blowes DW (2002) Acid neutralization mechanisms and metal release in mine tailing: a laboratory column experiment. *Geochim Coschim Acta* 66:1511–1523
- Karthe S, Szargan R, Suoninen E (1993) Oxidation of pyrite surface: a photoelectron spectroscopic study. *Appl Surf Sci* 72:157–170
- Lee CG, Chon HT, Jung MC (2001) Heavy metal contamination in the vicinity of the Daduk Au-Ag-Pb-Zn mine in Korea. *Appl Geochem* 16:1377–1386
- Lu L (2002) The study on surface reaction of pyrite (in Chinese with English abstract). Ph.D Thesis, Nanjing University
- Luther GW (1987) Pyrite oxidation and reduction: molecular orbital theory consideration. *Geochim Coschim Acta* 51:3193–3199
- Ma YG, Liu CQ (1999) Trace element geochemistry during chemical weathering: as exemplified by the weathering crust of granite, Longnan, Jiangxi, China. *Chin Sci Bull* 44:2260–2263
- Mcgregor RG, Blowes DW, Jambor JL (1998) The solid-phase controls on the mobility of heavy metals at the Copper Cliff tailing area, Sudbury, Ontario, Canada. *Jl of Contam Hydrol* 33:247–271
- Mckibben MA, Barnes HL (1986) Oxidation of pyrite in temperature acidic solution: Rate laws and surface textures. *Geochim Coschim Acta* 50:1509–1520
- Morin G, Ostergren JD, Juillot F, Hldefonse P, Calas G, Brown GE Jr (1999) XAFS determination of the chemical form of lead in smelter-contaminated soils and mine tailing: importance of adsorption processes. *Am Miner* 84:420–434

- Nesbitt HW, Muir IJ (1994) X-ray photoelectron spectroscopic studies of a pristine pyrite surface reacted with water vapour and air. *Geochim Coschim Acta* 58:4667–4679
- Nickson RT, Mearthur JM, Ravenscroft P, Burgess WG, Ahmed KM (2000) Mechanism of arsenic release to groundwater, Bangladesh and West Bengal. *Appl Geochem* 15:403–413
- Parkman RH, Charnock JM, Bryan ND, Livens FR, Vaughan DJ (1999) Reaction of copper and cadmium ions in solution with goethite, lepidocrocite, mackinawite, and pyrite. *Am Miner* 84:407–419
- Parsons MB, Bird DK, Einaudi MT, Alpers CN (2001) Geochemical and mineralogical controls on trace element release from the Penn Mine base-metal slag dump, California. *Appl Geochem* 16:1567–1593
- Pichler T, Hendry MJ, Hall GEM (2001) The mineralogy of arsenic in uranium mine tailings at the Rabbit Lake in-pit Facility, northern Saskatchewan, Canada. *Environ Geol* 40:495–506
- Pratt AR, Muir IJ, Nesbitt HW (1994a) X-ray photoelectron and Auger electron spectroscopic studies of pyrrhotite and mechanism of air oxidation. *Geochim Coschim Acta* 58:827–841
- Pratt AR, Nesbitt HW, Muir IJ (1994b) Generation of acids from mine waste: Oxidation leaching of pyrrhotite in dilute H₂SO₄ solutions at pH 3.0. *Geochim Coschim Acta* 58:5147–5159
- Rimstidt JD, Newcomb WD (1993) Measurement and analysis of rate data: The rate of reaction of ferric iron with pyrite. *Geochim Coschim Acta* 57:1919–1934
- Schaufuss AG, Nesbitt HW, Kartio I, Laajalehto K, Bancroft GM, Szargan R (1998) Incipient oxidation of fractured pyrite surfaces in air. *J Electron Spectrosc Relat Phenomen* 96:69–82
- Simma PH, Yanful EK, St-Arnaud L, Aube B (2000) A laboratory evaluation of metal release and transport in flooded pre-oxidized mine tailings. *Appl Geochem* 15:1245–1263
- Wang ZW, Zhou YZ, Zhang HH (1998) Characteristics and quantitative estimation in hydrothermal wall-rock alteration in Lianjiang silver-gold deposit, western Guangdong Province, South China (in Chinese with English abstract). *Geochimica* 27:251–257
- Williams TM, Smith B (2000) Hydrochemical characterization of acute acid mine drainage at Iron Duke mine, Mazowe, Zimbabwe. *Environl Geol* 39:272–278
- Williamson MA, Rimstidt JD (1994) The kinetics and electrochemical rate-determining step of aqueous pyrite oxidation. *Geochim Coschim Acta* 58:471–482
- Wu DQ, Peng JL, Chen GX, Yao DL, Xia Y (1996) Experimental study on adsorptions of metal ions onto sulfides—II. Influences of temperature and medium conditions. *Geochemica* 25:242–250 (in Chinese with English abstract)
- Wu DQ, Diao GY, Peng JL (1997) Experiment of the competition of metal ions onto minerals (in Chinese with English abstract). *Geochemica* 26:25–32
- Yu JY, Heo B (2001) Dilution and removal of dissolved metals from acid mine drainage along Imgok Creek, Korea. *Appl Geochem* 16:1041–1053
- Zhou YZ, Tu GZ, Chown ET (1994) Mathematical invariant and quantitative estimation on element migration of hydrothermal wall-rock alteration—with an example of application in the Hetai gold field, Guangdong Province, China. *Chin Sci Bull* 39:1638–1643